Synthesis and structural characterisation of $[Tp^{Me2}Nb(CH_3)_2(CH_3C{\equiv}CCH_3)]$ and $[Tp^{Me2}NbCl(CH_3)(CH_3C{\equiv}CCH_3)]$: is there an intrinsic α-agostic interaction in alkyl complexes of the $[Tp^{Me2}Nb(alkyne)]$ moiety?

Emmanuelle Teuma,[a] Michel Etienne,*[a] Bruno Donnadieu[a] and G. Sean McGrady*[b]

Received (in Durham, UK) 19th October 2005, Accepted 9th January 2006
First published as an Advance Article on the web 25th January 2006
DOI: 10.1039/b514820k

The methyl complexes $[Tp^{Me2}Nb(CH_3)_2(CH_3C{\equiv}CCH_3)]$ (**2**) and $[Tp^{Me2}NbCl(CH_3)(CH_3C{\equiv}CCH_3)]$ (**3**) have been prepared from the corresponding dichloride, and their structures investigated by X-ray diffraction. In each case, the Nb–CH_3 moiety displays a normal geometry in comparison with other methylniobium derivatives, with no evidence for the structural distortions which attend an α-agostic interaction. The NMR spectra of **2** and **3**, including those of the CH_2D isotopomers, also point to a conventional methyl–metal complex, with no isotopic perturbation of resonance which can signal agostic behaviour. Likewise, the IR spectra of the CH_3, CH_2D and CD_3 isotopomers of **2** and **3** indicate a conventional bonding situation, although the asymmetric Nb–CH_3 potential leads to two distinct ν^{is}_{CD} modes in the CH_2D spectrum. Taken together, these results lead us to conclude that there is no intrinsic α-agostic interaction in the methyl complexes **2** and **3**, and that the α-agostic structures deduced for their longer chain alkyl congeners are predominantly the result of steric interactions between the alkyl moiety and the bulky Tp^{Me2} ligand.

Introduction

Agostic interactions between a transition metal and an appended alkyl ligand have been the subject of enduring interest since their existence and significance was appreciated some two decades ago.[1] They play an important role on the reaction coordinate characterising fundamental chemical and catalytic processes such as olefin polymerisation and C–H bond activation.[2] Over the past decade, hydrotris(3,5-dimethylpyrazolyl)-boratoniobium alkyne complexes of the form $[Tp^{Me2}NbCl(R)(alkyne)]$ (R = alkyl) have provided several unique and fascinating examples of agostic systems, on account of an apparent competition between equally matched steric and electronic effects. Steric locking of the carbon chain of a primary alkyl group in the cleft between two pyrazole rings induces a preference for an α-CH agostic interaction with the niobium centre even when β-hydrogen atoms are present, as was observed for the ethyl complex $[Tp^{Me2}NbClEt(PhC{\equiv}CMe)]$.[3] If the ethyl ligand is replaced by an isopropyl moiety, there are two ways of fulfilling the steric requirements of the Tp^{Me2} ligand. One conformer can engage in the electronically preferable β-CH agostic interaction, whereas the other conformer directs the α-hydrogen towards the agostic site. Such a situation allows for competition between steric and electronic preferences, and has produced a unique example of an equilibrium between α-CH and β-CH agostic rotamers of a single alkyl group in the system $[Tp^{Me2}NbCl^{i}Pr(PhC{\equiv}CMe)]$.[3,4] Tethering together the arms of the secondary alkyl group to form a cycloalkyl derivative increases steric interactions with the pendant methyl groups of the Tp^{Me2} ligand and modifies the equilibrium preferences.[5] Even more striking is the observation of a unique case of an α-C–C agostic interaction in a cyclopropyl complex.[5,6] The preference of an α-C–C agostic structure over both α- and β-CH agostic ones is ascribed to the destabilisation and consequent activation of the C–C bond arising from the poor overlap of orbitals in the small C_3 ring.

Given the proclivity of these alkylniobium systems to display agostic structures, we were keen to remove the steric interaction between the alkyl chain and the Tp^{Me2} ligand, and to explore the structure of simple methyl derivatives of $[Tp^{Me2}NbCl_2(alkyne)]$ systems in which only electronic effects are at work. That steric effects cloud the picture in systems such as these is evident from the fact that the heavier Group 5 metal complex $[Tp^{Me2}TaCH_3(CH_2CH_3)(PhC{\equiv}CCH_3)]$ displays an α-CH agostic interaction with the methylene portion of the ethyl ligand, rather than with the methyl ligand itself.[7] The structurally and spectroscopically simple methyl group was at the heart of the early seminal work on agostic systems by Green and co-workers[8] and Calvert and Shapley[9] in mononuclear and polynuclear systems, respectively. In the last few years, great progress has been made in understanding the

[a] *Laboratoire de Chimie de Coordination du CNRS, UPR 8241, liée par conventions à l'Université Paul Sabatier et à l'Institut National Polytechnique de Toulouse, 205 Route de Narbonne, 31077 Toulouse, Cedex 4, France. E-mail: etienne@lcc-toulouse.fr*
[b] *Department of Chemistry, University of New Brunswick, Fredericton, Canada N.B. E3B 6E2. E-mail: smcgrady@unb.ca*

nature of agostic interactions in metal methyl complexes,[1,10,11] thanks to detailed analysis of NMR (both in solution[12] and in the solid state[13]) and IR spectra (usually for different isotopomers),[14–16] and theoretical investigations.[17–21] For d^0 systems, the amount of direct interaction between the metal centre and the agostic C–H bond itself (whether α or β) has been shown to be small, reorganisation of electron density over the entire alkyl group being responsible for the observed distortions.[11] In this respect, the case of the methyl ligand remains a challenge because of its high symmetry and small size, each of which complicate the analysis.

In this paper, we describe the syntheses and structural and spectroscopic characterisation of the dimethyl and (chloro)-methyl complexes $[Tp^{Me2}NbCl(CH_3)(CH_3C{\equiv}CCH_3)]$ and $[Tp^{Me2}Nb(CH_3)_2(CH_3C{\equiv}CCH_3)]$, including a study of the CH_2D and CD_3 isotopomers by NMR and IR spectroscopies. Detailed analysis of the spectroscopic data provides no evidence for an α-CH agostic interaction with the niobium centre in either complex, and leads us to conclude that the predominance of such α-agostic interactions in derivatives with longer-chain alkyl substituents is a consequence of the steric interactions within the coordination sphere of the metal, rather than of any electronic driving force at work in these systems.

Experimental

All experiments were carried out under an atmosphere of dry N_2 using conventional Schlenk tube or glove-box techniques. Solvents were dried by refluxing in a N_2 atmosphere over the appropriate drying agent: toluene, hexane, pentane, 1,4-dioxane (CaH_2), THF, Et_2O (sodium/benzophenone). $[Tp^{Me2}NbCl_2(CH_3C{\equiv}CCH_3)]$ **1**[22] and CH_2DCl[12] were synthesised according to published procedures. Lithium and magnesium derivatives were prepared according to classical procedures, except for $LiCH_3$ and CH_3MgCl in Et_2O, which were purchased (Aldrich). NMR solvents were freeze–pump–thawed three times and stored over molecular sieves under N_2. NMR spectra were measured using a Bruker AM 250, DPX 300 or AMX 400 spectrometer. Only pertinent $^1J_{CH}$ values are reported for the ^{13}C NMR spectra. If required, $^1J_{CH}$ values were measured from the ^{13}C satellites in the ^1H NMR spectra. Some assignments were confirmed with the aid of HMQC ^1H–^{13}C experiments. FTIR spectra were measured for samples contained in KBr pellets using a Perkin-Elmer 1725X spectrometer. X-Ray diffraction measurements of single crystals were made using an IPDS STOE diffractometer at 160 K. Elemental analyses were performed by the Analytical Service of the LCC.

$[Tp^{Me2}Nb(CH_3)_2(CH_3C{\equiv}CCH_3)]$ (2)

1 (0.257 g; 0.50 mmol) was dissolved in Et_2O (50 mL). To this cooled solution (0 °C), MeLi in Et_2O (0.7 mL of a 1.6 M solution; 1.1 mmol) was added dropwise with stirring. The initially purple solution turned orange then yellow over a period of 30 min. After *ca.* 1 h, the resulting slurry was filtered through a pad of Celite that was subsequently rinsed with pentane. The clear solution was pumped to dryness. Crystallisation from a toluene–pentane mixture (1/10 v/v) yielded orange crystals of **2** overnight that were collected by filtration, rinsed with cold pentane (0 °C) and dried *in vacuo*. Yield: 0.20 g, 0.42 mmol; 85%. Anal. Calc. for $C_{21}H_{34}BN_6Nb$: C 53.18, H 7.23, N 17.72%. Found: C 53.57, H 7.42, N 17.72%. ^1H NMR (C_6D_6, 200 MHz, 293 K) δ 5.79, 5.57 (both s, 1 : 2 H resp., $Tp^{Me2}CH$), 3.25 (s, 3 H, $\equiv CCH_3$), 2.48 (s, 3 H, $Tp^{Me2}CH_3$), 2.45 (s, 3 H, $\equiv CCH_3$), 2.24, 2.08, 1.89 (all s, 3 : 6 : 6 H resp., $Tp^{Me2}CH_3$), 1.05 (s, 6 H, $NbCH_3$). ^{13}C NMR (C_6D_6, 50 MHz, 297 K): δ 247.1, 231.6 ($\equiv CCH_3$), 151.3, 149.9, 143.7, 143.6 ($Tp^{Me2}CCH_3$); 106.9, 105.9 ($Tp^{Me2}CH$), 52.5 (br q, $^1J_{CH}$ 118 Hz, $w_{1/2}$ 5 Hz, $NbCH_3$), 21.9, 20.7 ($\equiv CCH_3$), 15.1, 14.5, 12.9, 12.7 ($Tp^{Me2}CH_3$).

$[Tp^{Me2}Nb(CH_2D)_2(CH_3C{\equiv}CCH_3)]$ (2-d_1)

2-d_1 was similarly obtained from **1** and 2 equivalents of $LiCH_2D$. ^1H NMR (C_7D_8, 400 MHz, 293 K): δ 6.01, 5.78 (both s, 1 : 2 H resp., $Tp^{Me2}CH$), 3.50 (s, 3 H, $\equiv CCH_3$), 2.70 (s, 3 H, $Tp^{Me2}CH_3$), 2.66 (s, 3 H, $\equiv CCH_3$), 2.34, 2.12 (all s, 3 : 12 H resp., $Tp^{Me2}CH_3$), 1.14 (br s, 4 H, $NbCH_2D$). $^{13}C\{^1H\}$ NMR (C_6D_6, 75 MHz , 300 K): δ 247.2, 231.7 ($\equiv CCH_3$), 151.4, 150.0, 143.7, 143.6 ($Tp^{Me2}CCH_3$), 108.1, 107.0 ($Tp^{Me2}CH$), 52.1 ($w_{1/2}$ 60 Hz, $NbCH_2D$), 21.9, 20.6 ($\equiv CCH_3$), 15.1, 14.5, 12.9, 12.7 ($Tp^{Me2}CH_3$).

$[Tp^{Me2}Nb(CD_3)_2(CH_3C{\equiv}CCH_3)]$ (2-d_3)

1 (0.257 g, 0.50 mmol) was dissolved in Et_2O (30 mL). To this cooled solution (0 °C), CD_3MgI in Et_2O (2.7 mL, 1.0 mmol) was added dropwise with stirring. The initially purple solution turned orange and a brownish precipitate appeared. Dioxane (1.5 mL) was added and the slurry filtered through a Celite pad that was then rinsed with pentane. Volatiles were removed *in vacuo* and the residue was extracted with pentane, filtered and evaporated to dryness. Crystallisation from toluene–pentane (1/10 v/v) yielded yellow–orange crystals of **2-d_3** that were collected by filtration, rinsed with cold pentane and dried *in vacuo*. Yield 0.190 g, 0.4 mmol; 80%. ^1H NMR (C_6D_6, 300 MHz , 300 K): δ 5.80, 5.57 (both s, 1 : 2 H resp., $Tp^{Me2}CH$), 3.27 (s, 3 H, $\equiv CCH_3$), 2.47 (s, 3 H, $Tp^{Me2}CH_3$), 2.44 (s, 3 H, $\equiv CCH_3$), 2.25, 2.10, 1.89 (all s, 3 : 6 : 6 H resp., $Tp^{Me2}CH_3$). $^{13}C\{^1H\}$ (C_6D_6, 75 MHz, 300 K): δ 247.1, 231.6 ($\equiv CCH_3$), 151.4, 149.9, 143.7 ($Tp^{Me2}CCH_3$), 108.1, 106.9 ($Tp^{Me2}CH$), 51 ($w_{1/2}$ 85 Hz, $NbCD_3$), 21.9, 20.6 ($\equiv CCH_3$), 15.1, 14.5, 12.9, 12.7 ($Tp^{Me2}CH_3$).

$[Tp^{Me2}NbCl(CH_3)(CH_3C{\equiv}CCH_3)]$ (3)

2 (0.237 g, 0.50 mmol) was dissolved in Et_2O (70 mL) and the solution was cooled to −70 °C. A solution of HCl in Et_2O (0.5 mL, 0.5 mmol) was then added dropwise. The initially yellow solution turned orange over the course of 30 min. After *ca.* 2 h at 0 °C, the volatiles were removed *in vacuo*. The residue was extracted with pentane, filtered and crystallisation from a toluene–pentane (1/10 v/v) mixture yielded **3** as orange crystals that were rinsed with pentane and dried *in vacuo*. Yield: 0.200 g; 0.40 mmol; 80%. Anal. Calc. for $C_{20}H_{31}BClN_6Nb$: C 48.56, H 6.32, N 16.99%. Found: C 48.62, H 5.87, N 16.65%. ^1H NMR (C_6D_6, 300 MHz, 300 K): δ 5.68, 5.53, 5.51 (all s, 1 H each, $Tp^{Me2}CH$), 3.36 (s, 3 H, $\equiv CCH_3$), 2.71, 2.17, 2.08, 2.05, 2.01, 1.75 (all s, 3 H each, $Tp^{Me2}CH_3$), 2.28 (s, 3 H, $\equiv CCH_3$), 1.65 (s, 3 H, $NbCH_3$). ^1H NMR (CD_2Cl_2, 400 MHz, 293 K): δ 5.98, 5.88, 5.81 (all s, 1 H each, $Tp^{Me2}CH$), 3.30 (s, 3 H,

≡CCH_3), 2.50, 2.46, 2.44, 2.42, 1.95, 1.82 (all s, 3 H each, CH_3 de Tp^{Me2}), 2.34 (s, 3 H, ≡CCH_3), 1.20 (s, 3 H, NbCH_3). ^{13}C NMR (C_6D_6, 75 MHz, 300 K): δ 250.6, 230.0 (≡CCH$_3$), 152.7, 152.3, 149.6, 144.3, 143.9 ($Tp^{Me2}$$CCH_3$), 108.4, 107.8, 107.6 ($Tp^{Me2}$$C$H), 60.6 (br q, $^1J_{CH}$ 123 Hz, $w_{1/2}$ 5 Hz, NbCH$_3$), 22.1, 21.5 (≡CCH$_3$), 15.6, 15.4, 14.7, 13.1, 12.9, 12.6 ($Tp^{Me2}$$CCH_3$).

[Tp^{Me2}NbCl(CH_2D)($CH_3C{\equiv}CCH_3$)] (3-d_1)

3-d_1 was prepared similarly in 75% yield from **2-d_1** and HCl in Et_2O. ^{1}H NMR (CD_2Cl_2, 400 MHz, 293 K): δ 5.95, 5.86, 5.80 (all s, 1 H each, Tp^{Me2}CH), 3.28 (s, 3 H, ≡CCH_3), 2.47, 2.43, 2.42, 2.39, 1.93, 1.79 (all s, 3 H each, CH_3 de Tp^{Me2}), 2.31 (s, 3 H, ≡CCH_3), 1.11 (d, 1 H, $^2J_{HH}$ 11 Hz, NbCH_2D), 1.10 (d, 1 H, $^2J_{HH}$ 11 Hz, NbCH_2D). ^{13}C{^{1}H} NMR (CD_2Cl_2, 100 MHz, 293 K): δ 251.5, 231.3 (≡CCH$_3$), 151.5, 151.2, 148.9, 144.1, 143.9, 143.5 ($Tp^{Me2}$$CCH_3$), 107.1, 106.5, 106.4 ($Tp^{Me2}$$C$H), 59 ($w_{1/2}$ 100 Hz, NbCH$_3$), 21.2, 20.4 (≡CCH$_3$), 14.1, 13.9, 13.6, 12.3, 12.0, 11.8 ($Tp^{Me2}$$CH_3$).

[Tp^{Me2}NbCl(CD_3)($CH_3C{\equiv}CCH_3$)] (3-d_3)

3-d_3 was prepared similarly in 80% yield from **2-d_3** and HCl in Et_2O. ^{1}H NMR (C_6D_6, 300 MHz, 300 K): δ 5.68, 5.53, 5.51 (all s, 1 H each, Tp^{Me2}CH), 3.36, 2.28 (both s, ≡CCH_3), 2.71, 2.17, 2.07, 2.05, 2.02, 1.75 (all s, 3 H each, CH_3 de Tp^{Me2}). ^{13}C{^{1}H} NMR (C_6D_6; 75 MHz; 300 K): δ 250.6, 230.0 (≡CCH$_3$), 152.5, 149.4, 143.7 ($Tp^{Me2}$$CCH_3$), 108.2, 107.6, 107.3 ($Tp^{Me2}$$C$H), 59 ($w_{1/2}$ 140 Hz, NbCH$_3$), 21.9, 21.3 (≡CCH$_3$), 15.4, 15.2, 14.4, 12.9, 12.6, 12.4 ($Tp^{Me2}$$CH_3$).

X-Ray structure determinations

Measurements were performed at T = 160(2) K using a one-circle STOE Imaging Plate Detector X-ray diffractometer system (Mo-radiation, λ = 0.710 73 Å). A phi scan strategy was used for the data collection, and frames were integrated using the STOE software package X-RED;[23] the integrated frames yielded the following:

[Tp^{Me2}Nb(CH_3)$_2$($CH_3C{\equiv}CCH_3$)] (2)

$C_{21}H_{34}BN_6Nb$: M = 474.26; 15009 reflections collected at a maximum 2θ angle of 49.40° (3828 independent, R_{int} = 0.0547, R_{sig} = 0.0391, completeness = 99.8%) and 3293 (86.02%) reflections were found greater than 2σ(I); orthorhombic, space group $Pca2_1$, unit cell parameters: a = 10.1222(13), b = 13.6129(13), c = 16.5563(15) Å, V = 2281.3(4) Å^3, Z = 4, D_c = 1.381 Mg m^{-3}.

[Tp^{Me2}NbCl(CH_3)($CH_3C{\equiv}CCH_3$)] (3)

$C_{20}H_{31}BClN_6Nb$: M = 494.68; 14461 reflections collected at a maximum 2θ angle of 48.80° (3579 independent, R_{int} = 0.1253, R_{sig} = 0.0977, completeness = 98.7%) and 2337 (65.29%) reflections were found greater than 2σ(I); orthorhombic, space group $Pca2_1$; unit cell parameters: a = 10.0681(14), b = 13.6445(12), c = 16.4959(13) Å, V = 2266.1(4) Å^3, Z = 4, D_c = 1.450 Mg m^{-3}.

Absorption corrections were applied to all data using the DIFABS program.[24] SIR92 [25] and SHELXL 97 [26] included in the WinGX software package [27] used for phase determination and structure refinement, respectively. Direct methods of phase determination followed by a difference Fourier plot led to an electron density map from which most of the non-hydrogen atoms were found. With subsequent isotropic refinement and Fourier difference synthesis, all of the non-hydrogen atoms could be identified. Atomic coordinates and isotropic and anisotropic displacement parameters of all non-hydrogen atoms were refined by means of a full-matrix least-squares procedure on F^2. H-Atoms were included in the refinement in calculated positions, riding on the carbon atoms with an isotropic thermal parameter fixed 20% higher than the carbon atom to which they were attached. In the case of methyl groups, torsion angles were also refined. Specific hydrogens connected to B(1) atoms were isotropically refined. For complex **3**, disorder exists between the methyl group and the chlorine atom bound to niobium, leading to two isomers in the same asymmetric unit. Electronic density residues fit with a model in which one CH_3 group and one Cl atom bound to Nb are located on either side of the NbC_2 metallacycle. All atoms involved in the disorder were anisotropically refined with a ratio of occupancy found to be close to 60/40%. The refinement process converged for **2** at $R1$ = 0.0318, $wR2$ = 0.0745 with intensity, $I > 2\sigma(I)$. The largest peak/hole in the final difference map was between 0.674 and −0.540 e Å^{-3}; for **3**, refinement converged at $R1$ = 0.0473, $wR2$ = 0.0892 with intensity, $I > 2\sigma(I)$. The largest peak/hole in the final difference map was between 0.683 and −0.482 e Å^{-3}. All calculations were carried out using WinGX 32,[27] and plots were drawn using the software ORTEP32.[28]

CCDC reference numbers 286983 and 286984.

For crystallographic data in CIF or other electronic format see DOI: 10.1039/b514820k

Results and discussion

Synthesis

Reaction of [Tp^{Me2}NbCl$_2$($CH_3C{\equiv}CCH_3$)] (**1**) with two equivalents of LiCH_3 in Et_2O proceeds cleanly to give [Tp^{Me2}Nb(CH_3)$_2$($CH_3C{\equiv}CCH_3$)] (**2**) in 80% yield after work-up and crystallisation (Scheme 1). A similar straightforward synthesis has been reported previously for [Tp^{Me2}Nb(CH_3)$_2$(PhC≡CCH$_3$)][22] and related cyclopentadienyl derivatives.[29] Interestingly, the Grignard reagent CH_3MgCl is not as efficient as an alkylating agent, and some unreacted **1** remained in solution after several hours, even when a slight excess of the Grignard reagent is employed. Addition of 1,4-dioxane shifts the equilibrium in Scheme 1 towards the formation of **2** and makes its separation easier. The partially

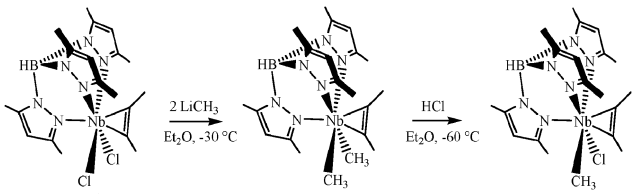

Scheme 1

deuteriated derivative $[Tp^{Me2}Nb(CH_2D)_2(CH_3C{\equiv}CCH_3)]$ (**2-d$_1$**) was similarly obtained from **1** and two equivalents of $LiCH_2D$ in Et_2O. The fully deuteriated dimethyl complex $[Tp^{Me2}Nb(CD_3)_2(CH_3C{\equiv}CCH_3)]$ (**2-d$_3$**) was obtained from **1** and two equivalents of CD_3MgI in Et_2O containing 1,4-dioxane.

The synthesis of the (chloro)methyl complex $[Tp^{Me2}NbCl(CH_3)(CH_3C{\equiv}CCH_3)]$ (**3**) proved more challenging. Addition of one equivalent of $LiCH_3$ to **1** in Et_2O at −80 °C resulted in an approximate 1 : 1 mixture of **1** and **2**, with only traces of the desired monomethyl complex. The use of CH_3MgCl under kinetically controlled conditions improved the ratio, but only to *ca.* 70% of **1** and 15% each of **2** and **3**. Accordingly, alternative routes to **3** were investigated starting from **2**. Addition of one equivalent of Me_3SiCl to **2** again produced a mixture of **2** and **3**. Eventually, we found that addition of one equivalent of HCl (as an ethereal solution) to **1** at –60 °C produced the desired (chloro)methyl complex **3** cleanly; Scheme 1. The isotopomers $[Tp^{Me2}NbCl(CH_2D)(CH_3C{\equiv}CCH_3)]$ (**3-d$_1$**) and $[Tp^{Me2}NbCl(CD_3)(CH_3C{\equiv}CCH_3)]$ (**3-d$_3$**) were each obtained in a similar fashion from **2-d$_1$** and **2-d$_3$**, respectively.

X-Ray crystal structures

The structures of **2** and **3** (Fig. 1) as determined by single-crystal X-ray diffraction at 160 K reveal a conventional distorted octahedral coordination environment around the niobium atom, if the alkyne ligand is considered to occupy a single coordination site.

The structure of **3** displays approximately statistical disorder (60 : 40) between the niobium-bound chlorine and methyl carbon atoms, precluding a detailed analysis of the Nb–Cl and Nb–CH_3 bond lengths and the Cl–Nb–CH_3 bond angle in this complex. Salient parameters with regard to the nature of the metal–methyl moieties are the Nb–CH_3 bond lengths and the CH_3–Nb–CH_3 angle for **2**. With values of 2.208(4) and 2.212(4) Å for Nb–C(10) and Nb–C(20), respectively, the Nb–C bonds appear perfectly normal. The C(10)–Nb–C(20) angle of 107.67(16)° is also unremarkable. In spite of the larger size of the alkyl groups in $[Tp^{Me2}NbCl(CH_2SiMe_3)(PhC{\equiv}CCH_3)]$[30] and $[Tp^{Me2}NbCl(c\text{-}C_5H_9)(CH_3C{\equiv}CCH_3)]$,[5] the presence of an α-agostic interaction with the alkyl ligand in these systems leads to somewhat shorter Nb–C distances of 2.204(4) and 2.174(4) Å, respectively. The agostic methyl cation $[Tp^{Me2}Nb\text{-}CH_3(OEt_2)(CH_3C{\equiv}CCH_3)]^+$ is characterised by a Nb–C bond length of 2.182(7) Å.[31] The Nb–C bonds in **2** are also similar to those in other dialkyl derivatives of niobium, such as the cyclopentadienyl analogue $[(\eta^5\text{-}C_5H_4SiMe_3)Nb(CH_2SiMe_3)_2(Me_3SiC{\equiv}CSiMe_3)]$ [2.193(6) and 2.198(6) Å],[32] and the mixed (chloro)methylniobium(v) compounds Me_2NbCl_3 and Me_3NbCl_2 [2.135(9) and 2.148(4) Å], as determined in the gas phase by electron diffraction.[33] Slightly shorter M–C bonds of 2.169(6) and 2.181(6) Å were observed for the tantalum benzyne derivative $[(\eta^5\text{-}C_5Me_5)Ta(CH_3)_2(C_6H_4)]$.[34] The X–Nb–X′ angle in $[Tp^{Me2}NbXX'(alkyne)]$ systems tends to increase in agostic complexes: in $[Tp^{Me2}NbCl_2(PhC{\equiv}CCH_3)]$, the Cl–Nb–Cl angle is 102(1)°,[35] whereas in the α-CH agostic systems $[Tp^{Me2}NbCl(CH_2SiMe_3)(PhC{\equiv}CCH_3)]$ and $[Tp^{Me2}NbCl(c\text{-}C_5H_9)(CH_3C{\equiv}CCH_3)]$, the C–Nb–Cl angle is 104.3(1) and 108.9(1)°, respectively.[5,30] For the unique α-C–C agostic $[Tp^{Me2}NbCl(c\text{-}C_3H_5)(CH_3C{\equiv}CCH_3)]$, the corresponding angle is significantly larger at 110.85(8)°,[5,6] albeit still much less than the value of 122.1(1)° in the β-CH agostic system $[Tp^{Me2}NbCl(i\text{-}C_3H_7)(PhC{\equiv}CCH_3)]$.[3] This anomalously large angle has also been ascribed to secondary π-interactions[36] and to better overlap between metal- and alkyne-based orbitals.[32] In summary, the X-ray crystal structures of **2** and **3** offer no evidence for the existence of α-agostic interactions between the niobium centre and its appended methyl ligands.

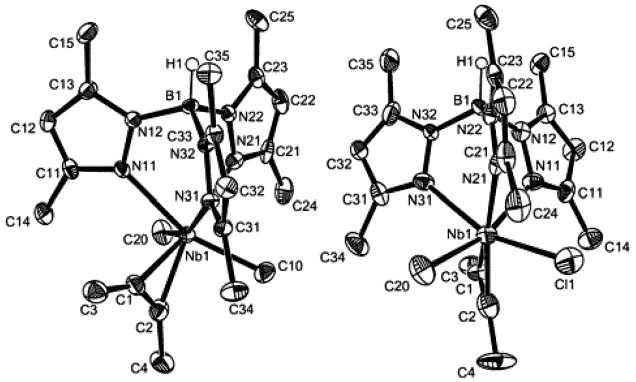

Fig. 1 Molecular structures of $[Tp^{Me2}Nb(CH_3)_2(CH_3C{\equiv}CCH_3)]$ (**2**) and $[Tp^{Me2}NbCl(CH_3)(CH_3C{\equiv}CCH_3)]$ (**3**), as determined by single-crystal X-ray diffraction at 160 K. Selected bond distances (Å) and angles (°) with esds in parentheses. For **2**: Nb(1)–C(1) 2.044(4), Nb(1)–C(2) 2.053(4), Nb(1)–C(10) 2.208(4), Nb(1)–C(20) 2.212(4), Nb(1)–N(31) 2.312(3), Nb(1)–N(21) 2.337(3), Nb(1)–N(11) 2.340(3), C(1)–C(2) 1.305(6); C(10)–Nb(1)–C(20) 107.67(16), C(3)–C(1)–Nb(1) 144.7(3), C(4)–C(2)–Nb(1) 146.8(3). For **3**: Nb(1)–C(1) 2.086(10), Nb(1)–C(2) 2.051(10), C(1)–C(2) 1.321(12); Cl(1)–Nb(1)–C(20) 104.39(15). Owing to statistical disorder between Cl(1) and C(20) positions in the structure of **3**, bond distances involving these atoms are subject to large uncertainties.

NMR spectroscopic studies

In their ^1H and ^{13}C NMR spectra, **2** and **3** show the usual symmetrical and unsymmetrical patterns, respectively, for the proton and carbon resonances of the Tp^{Me2} ligand. In benzene-d_6, the equivalent niobium-bound methyl groups of **2** exhibit a singlet in the ^1H NMR spectrum at δ 1.05 and a broad ($w_{1/2}$ = 5 Hz) quartet in the ^{13}C NMR spectrum at δ 52.5 ($^1J_{CH}$ = 118 Hz). A value of 120 Hz is also measured for $^1J_{CH}$ from the ^{13}C satellites in the ^1H NMR spectrum. These values do not vary significantly in the temperature range 193–343 K in toluene-d_8. For **3**, the electronegative chloro ligand causes these resonances to shift to higher frequency: the methyl group ^1H nuclei of **2** appear as a singlet at δ 1.65 and the ^{13}C nucleus of the methyl group resonates at δ 60.6 with $^1J_{CH}$ = 123 Hz ($w_{1/2}$ 6 Hz), or 121 Hz if measured from the ^1H NMR spectrum. These chemical shifts and coupling constants are entirely normal for anagostic metal–methyl moieties.

Isotopic perturbation of resonance (IPR)[37] is a powerful and sensitive technique, which has been applied to a variety of methyl–metal compounds to probe for α-agostic interactions,

albeit with chequered results.[9,12] The technique involves partial deuteriation of the methyl ligand; a thermodynamic preference for the deuteron to occupy the bridging agostic site leads to a temperature-dependent chemical shift difference, $\Delta\delta = \delta(CH_3) - \delta(CH_2D)$ between the labelled and unlabelled isotopomers of the agostic methyl moiety. As expected, the deuteriation of one of the three C–H bonds of the methyl group(s) of **2** and **3** causes both the ^1H and ^{13}C NMR resonances to move to lower frequency, and further broadens the ^{13}C NMR signal on account of the quadrupole moment of deuterium. For example, at room temperature the niobium-bound carbons of **2-d$_1$** display a $^{13}C\{^1H\}$ signal at δ 52.1 with $w_{1/2}$ = 60 Hz, and those of **2-d$_3$** resonate at δ 51.0 with $w_{1/2}$ = 85 Hz. Interestingly, for the isotopomers **2-d$_1$** and **3-d$_1$**, the hydrogen nuclei of the NbCH_2D groups are diastereotopic, resulting in an AB-type ^1H NMR spectrum for each of these complexes; moreover, these spectra vary slightly with temperature. An expanded region of the 400 MHz ^1H NMR spectrum of **3-d$_1$** in dichloromethane-d_2 is shown in Fig. 2. From the base temperature of 193 K, the spectrum of NbCH_2D evolves from AB-type with $^2J_{HH}$ = 11 Hz and $\Delta\delta$ = 0.06 ppm, to almost A_2-type at 293 K. These modest but significant changes are not indicative of a site exchange phenomenon since there is no coalescence, the protons being diastereotopic. However, it indicates that the protons of the NbCH_2D moiety experience an averaged environment as the temperature is increased. In other words, there exists a barrier to rotation about the Nb–CH_2D bond (*q.v.*). Clearly this barrier is low, since the changes are small and occur over a wide temperature range. Furthermore, the small magnitude of $\Delta\delta$ at low temperature implies that the environments of the diastereotopic protons are chemically rather similar. The $\Delta\delta$ value of 0.06 ppm measured for **3** is an order of magnitude smaller than those reported for $[(\eta^5\text{-}C_5Me_4Et)WMe_4]^{+}$[12] and $[Os_3(CO)_{10}(H)Me]$,[9] and is characteristic of a secondary isotope effect.[37] In addition, there is virtually no change (*ca.* 0.03 ppm) in $\Delta\delta$ over the 100 K temperature range of the experiment. Taken together, these observations speak for the absence of agostic interactions in **2** and **3**,[12] although the limitations of the IPR technique in identifying agostic interactions in early transition metal alkyl systems are well documented.[13]

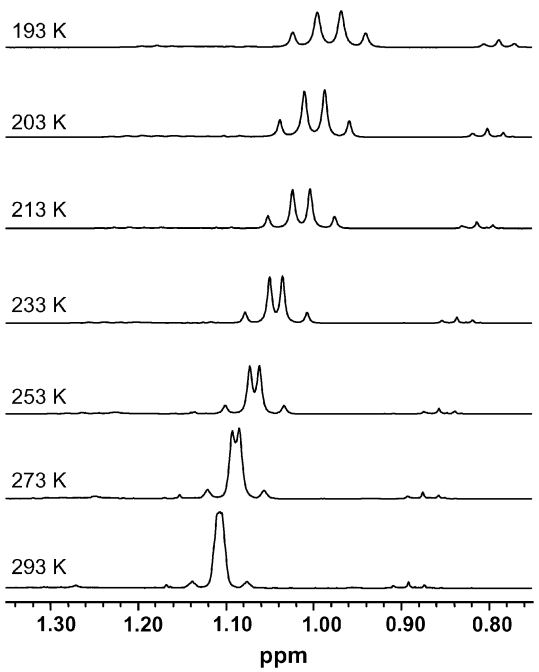

Fig. 2 Expanded region of the ^1H NMR spectrum (dichloromethane-d_2, 400 MHz) of $[Tp^{Me2}NbCl(CH_2D)(CH_3C{\equiv}CCH_3)]$ **(3-d$_1$)** over the temperature range 193–293 K.

IR spectroscopic studies

While it is now generally accepted that the C–H bond elongation which attends agostic interactions in early transition metal complexes is modest,[11] the partial deuteriation technique developed by McKean[38] remains a powerful and very sensitive yardstick of the internal geometry of the alkyl ligand in such situations. The technique has been applied to a wide range of transition-metal alkyl species to investigate the geometry of the M–R moiety.[14–16,39,40] When the barrier to internal rotation is greater than about 4 kJ mol^{-1}, inequivalent C–H bonds in a methyl group can be independently observed in the IR spectrum: a particularly useful tool for identifying agostic interactions. The technique exploits the difference in the bond stretching frequencies between C–H and C–D moieties: the large increase in reduced mass when deuterium replaces the lighter isotope effectively decouples the oscillators from one another, leading to the observation of an isolated C–H stretching vibration, ν^{is}_{CH}, in the IR spectrum of a CHD_2 compound and a ν^{is}_{CD} feature in the corresponding CH_2D one. Empirical correlations link ν^{is} with the bond length r_0(CH) and with its dissociation energy D_0,[38] allowing an accurate assessment of the C–H and C–D bond strengths in a methyl group.

The IR spectra of **2** and **3** and their **d$_1$** and **d$_3$** isotopomers in the νCH and νCD region are presented in Fig. 3. Unfortunately, the νCH vibrations of the metal-methyl moieties in **2** and **3** are obscured by the manifold of features arising from the Tp^{Me2} and 2-butyne ligands, which fall between 2850 and 3000 cm^{-1}. However, the CH_2D isotopomers **2-d$_1$** and **3-d$_1$** allow access to important structural information through the observation of two distinct ν^{is}_{CD} features for each complex. These occur at 2177 and 2160 cm^{-1} for **2-d$_1$**, and at 2192 and 2168 cm^{-1} for **3-d$_1$**; they reveal asymmetry in the methyl groups in each case.

The complex nature of the C–H stretching region of the spectrum for **2** and **3** has prevented us from applying the sum rule developed by McKean.[38] This would have allowed us to determine whether there are two stronger and one weaker bond in each methyl group, or *vice versa*. However, the ν^{is}_{CD} values at our disposal permit us to make other valuable deductions. In the diatomic approximation and with due allowance for anharmonicity, they can be converted to the corresponding ν^{is}_{CH} values by consideration of the relative reduced masses of the C–H and C–D oscillators: direct measurement of ν^{is}_{CH} is virtually impossible for **2** and **3**, on account of the large number of C–H moieties in the $Tp^{Me2}$and 2-butyne ligands (*q.v.*). This procedure yields ν^{is}_{CH} values of

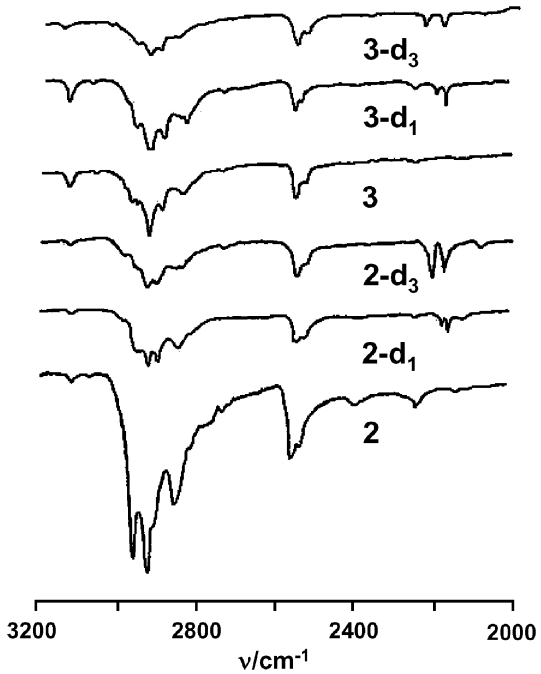

Fig. 3 IR spectrum (KBr pellet) of $[Tp^{Me2}Nb(CH_3)_2(CH_3C{\equiv}CCH_3)]$ (**2**); $[Tp^{Me2}Nb(CH_2D)_2(CH_3C{\equiv}CCH_3)]$ (**2-d$_1$**); $[Tp^{Me2}NbCl(CD_3)_2(CH_3C{\equiv}CCH_3)]$ (**2-d$_3$**); $[Tp^{Me2}NbCl(CH_3)(CH_3C{\equiv}CCH_3)]$ (**3**); $[Tp^{Me2}NbCl(CH_2D)(CH_3C{\equiv}CCH_3)]$ (**3-d$_1$**) and $[Tp^{Me2}NbCl(CD_3)(CH_3C{\equiv}CCH_3)]$ (**3-d$_3$**) in the region 3200–2000 cm^{-1}.

2934 and 2911 cm^{-1}, and 2954 and 2922 cm^{-1} for **2** and **3**, respectively.

The first point to note is that these values are characteristic of perfectly normal C–H bonds, as found in a range of methyl–metal complexes of the transition metals,[14–16,39,40] and are not indicative of any significant chemical change wrought by a M···H–C interaction, as is observed, for example, in the textbook β-agostic complex $[EtTiCl_3(dmpe)]$ (ν^{is}_{CH} = 2585 cm^{-1}),[41] or even of a modest α-agostic interaction as was proposed to exist in the molecule $[(\eta^5\text{-}C_5H_5)TiMe_3]$ (ν^{is}_{CH} = 2905 cm^{-1}).[15] The C–H bond distances for the metal-bound methyl groups in **2** and **3** can be estimated from the very accurate correlation reported by McKean.[38] This yields r_0(CH) values of 1.098 and 1.100, and 1.096 and 1.099 Å for **2** and **3**, respectively, and indicates bond strength differences of around 10 kJ mol^{-1} within each methyl group. In other words, although asymmetry exists in the methyl groups it is small, and well below the limits of detection of even neutron diffraction, the most accurate direct structural technique available for determining C–H bond distances. This asymmetry does not arise through any chemical perturbation of the methyl groups by the neighbouring metal centre; rather is it a consequence of the asymmetric potential experienced by the Nb–CH_2D rotor, as depicted for complex **3** in Scheme 2. The difference, $\Delta\nu$, in the two ν^{is}_{CH} values observed for **2** and **3** (23 and 32 cm^{-1}, respectively) is comparable with the corresponding value of 17 cm^{-1} found for $[(\eta^5\text{-}C_5H_5)_2TiMe_2]$,[39] which was also ascribed to an asymmetric methyl rotational potential rather than to any electronic effect. These $\Delta\nu$ values are much

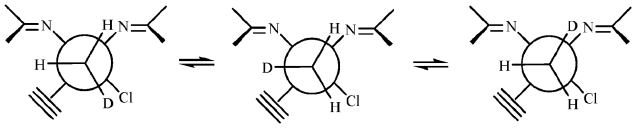

Scheme 2

smaller than those found for organic molecules such as Me_3N and Me_2O (> 100 cm^{-1}), in which individual C–H bonds in a methyl group lie either *trans* or *gauche* to a lone pair of electrons,[38] with the former experiencing a significant weakening related to the well known anomeric effect.[42]

Summary

The methylniobium complexes $[Tp^{Me2}Nb(CH_3)_2(CH_3C{\equiv}CCH_3)]$ **2** and $[Tp^{Me2}NbCl(CH_3)(CH_3C{\equiv}CCH_3)]$ **3** have each been synthesised and subjected to a thorough structural investigation, with the aim of determining whether or not α-agostic interactions are an intrinsic feature of the ground state of complexes of the type $[Tp^{Me2}NbCl_xR_{2-x}(alkyne)]$. Whilst the hydrogen atoms of the Nb–CH_3 moieties of **2** and **3** cannot be located precisely from the single-crystal X-ray studies, the Nb–C bond lengths and C–Nb–X bond angles provide no evidence of the distortions characteristic of α-agostic structures. The ^{1}H NMR spectra of **2** and **3** are normal, and those of their CH_2D-substituted isotopomers **2-d$_1$** and **3-d$_1$** reveal a small IPR effect characteristic of classical methyl groups. The IR spectra of **2** and **3**, along with those of their **d$_1$** and **d$_3$** isotopomers provide perhaps the most definitive evidence for the normal behaviour of the methyl moieties in these systems: they reveal an asymmetric potential about the Nb–C bond, but otherwise report a chemically unremarkable environment for the C–H bonds of the methyl groups. We conclude that there are no intrinsic α-agostic interactions in **2** and **3**, and that significant steric interactions between the alkyl and Tp^{Me2} ligands are predominantly responsible for the α-agostic structures which have been proven or inferred from X-ray diffraction and NMR spectroscopy for the longer-chain alkyl congeners of these systems.

Acknowledgements

We are grateful to the RSC and the Universite Paul Sabatier, Toulouse, for the provision of travel grants (to M. E.).

References

1 M. Brookhart, M. L. H. Green and L.-L. Wong, *Prog. Inorg. Chem.*, 1988, **36**, 1.
2 (*a*) H. H. Brintzinger, D. Fischer, R. Müllhaupt, B. Rieger and R. M. Waymouth, *Angew. Chem., Int. Ed. Engl.*, 1995, **34**, 1143; (*b*) R. H. Crabtree, *Angew. Chem., Int. Ed. Engl.*, 1993, **32**, 789.
3 (*a*) J. Jaffart, M. Etienne, F. Maseras, J. E. McGrady and O. Eisentein, *J. Am. Chem. Soc.*, 2001, **123**, 6000; (*b*) M. Etienne, *Organometallics*, 1994, **13**, 410.
4 J. Jaffart, R. Mathieu, M. Etienne, J. E. McGrady, O. Eisenstein and F. Maseras, *Chem. Commun.*, 1998, 2011.
5 J. Jaffart, M. L. Cole, M. Etienne, M. Reinhold, J. E. McGrady and F. Maseras, *Dalton Trans.*, 2003, 4057.

6 J. Jaffart, M. Etienne, M. Reinhold, J. E. McGrady and F. Maseras, *Chem. Commun.*, 2003, 876.
7 J.-C. Hierso and M. Etienne, *Eur. J. Inorg. Chem.*, 2000, 839.
8 Z. Dawoodi, M. L. H. Green, V. S. B. Mtetwa, K. Prout, A. J. Schultz, J. M. Williams and T. F. Koetzle, *J. Chem. Soc., Dalton Trans.*, 1986, 1629.
9 R. B. Calvert and J. R. Shapley, *J. Am. Chem. Soc.*, 1978, **100**, 7726.
10 R. H. Grubbs and G. W. Coates, *Acc. Chem. Res.*, 1996, **29**, 85.
11 W. Scherer and G. S. McGrady, *Angew. Chem., Int. Ed.*, 2004, **43**, 1782.
12 M. L. H. Green, A. K. Hughes, N. A. Popham, A. H. H. Stevens and L.-L. Wong, *J. Chem. Soc., Dalton Trans.*, 1992, 3077.
13 D. C. Maus, V. Copié, B. Sun, J. M. Griffiths, R. G. Griffin, S. Luo, R. R. Schrock, A. H. Lûu, S. W. Seidel, W. M. Davis and A. Groham, *J. Am. Chem. Soc.*, 1996, **118**, 5665.
14 D. C. McKean, G. P. McQuillan, I. Torto, N. C. Bednall, A. J. Downs and J. M. Dickinson, *J. Mol. Struct.*, 1991, **247**, 73.
15 G. S. McGrady, A. J. Downs, J. M. Hamblin and D. C. McKean, *Organometallics*, 1995, **14**, 3783.
16 G. S. McGrady, A. J. Downs, N. C. Bednall, D. C. McKean, W. Thiel, V. Jonas, G. Frenking and W. Scherer, *J. Phys. Chem. A*, 1997, **101**, 1951.
17 R. J. Goddard, R. Hoffmann and E. D. Jemmis, *J. Am. Chem. Soc.*, 1980, **102**, 7667.
18 O. Eisenstein and Y. Jean, *J. Am. Chem. Soc.*, 1985, **107**, 1177.
19 S. Obara, N. Koga and K. Morokuma, *J. Organomet. Chem.*, 1984, **270**, C33.
20 T. K. Woo, L. Fan and T. Ziegler, *Organometallics*, 1994, **13**, 2252.
21 H. Kawamura-Kuribayashi, N. Koga and K. Morokuma, *J. Am. Chem. Soc.*, 1992, **114**, 2359.
22 M. Etienne, F. Biasotto, R. Mathieu and J. L. Templeton, *Organometallics*, 1996, **15**, 1106.
23 Stoe, *X-RED*, Data Reduction for STADI4 and IPDS, Revision 1.08, Stoe & Cie, Darmstadt, Germany, 1996.
24 N. Walker and D. Stuart, *Acta Crystallogr., Sect. A*, 1983, **39**, 158.
25 A. Altomare, G. Cascarano, C. Giacovazzo and A. Guagliardi, *J. Appl. Crystallogr.*, 1993, **26**, 343.
26 SHELXTL Software Reference Manual, Version 6.10, Bruker Analytical X-ray System, Inc., Madison, WI, Dec. 5th 2000.
27 L. J. Farrugia, *J. Appl. Crystallogr.*, 1999, **32**, 837.
28 L. J. Farrugia, *J. Appl. Crystallogr.*, 1997, **30**, 565.
29 M. D. Curtis, J. Real, W. Hirpo and W. M. Butler, *Organometallics*, 1990, **9**, 66.
30 M. Etienne, B. Donnadieu and R. Mathieu, *J. Am. Chem. Soc.*, 1997, **119**, 3218.
31 H. M. Pritchard, L. Vendier, M. Etienne and G. S. McGrady, *Organometallics*, 2004, **23**, 1203.
32 A. Galindo, M. Gomez, P. Gomez-Sal, A. Martin, D. del Rio and F. Sanchez, *Organometallics*, 2002, **21**, 293.
33 G. S. McGrady, A. Haaland, H.-P. Verne, H.-V. Volden, A. J. Downs, D. Shorokhov, G. Eickerling and W. Scherer, *Chem.–Eur. J.*, 2005, **11**, 4921.
34 M. R. Churchill and W. J. Youngs, *Inorg. Chem.*, 1979, **18**, 2454.
35 M. Etienne, P. S. White and J. L. Templeton, *Organometallics*, 1991, **10**, 3801.
36 M. Etienne, B. Donnadieu, R. Mathieu, J. Fernandez-Baeza, F. Jalon, A. Otero and M.-E. Rodrigo-Blanco, *Organometallics*, 1996, **15**, 4597.
37 R. K. Harris, *Nuclear Magnetic Resonance Spectroscopy*, Longman, London, 1986, p. 194.
38 (*a*) D. C. McKean, *Chem. Soc. Rev.*, 1978, **7**, 399; (*b*) D. C. McKean, *Croat. Chem. Acta*, 1988, **61**, 447.
39 G. P. McQuillan, D. C. McKean and I. Torto, *J. Organomet. Chem.*, 1986, **312**, 183.
40 D. C. McKean, G. P. McQuillan and D. W. Thompson, *Spectrochim. Acta, Part A*, 1980, **36**, 1009.
41 (*a*) G. S. McGrady, A. J. Downs, A. Haaland, W. Scherer and D. C. McKean, *Chem. Commun.*, 1997, 1547; (*b*) D. C. McKean, G. S. McGrady, A. J. Downs, W. Scherer and A. Haaland, *Phys. Chem. Chem. Phys.*, 2001, **3**, 2781.
42 J. O. Williams, J. N. Scarsdale, L. Schäfer and H. J. Geise, *J. Mol. Struct.*, 1981, **76**, 11.